Supporting Information

A MOF-derived Carbon Host Associated with Fe and Co Single Atoms for Li-Se Batteries

*Yuqing Cao[a], Feifei Lei[a], Yunliang Li[a], Shilun Qiu[a], Yan Wang[b], Wei Zhang[b] and Zongtao Zhang[a]**

[a]State Key Laboratory of Inorganic Synthesis and Preparative Chemistry, College of Chemistry, Jilin University, Changchun 130012, China

[b]Electron Microscopy Center, Jilin University, Changchun 130012, China

*Corresponding author

E-mail: zzhang@jlu.edu.cn(Z. Zhang)

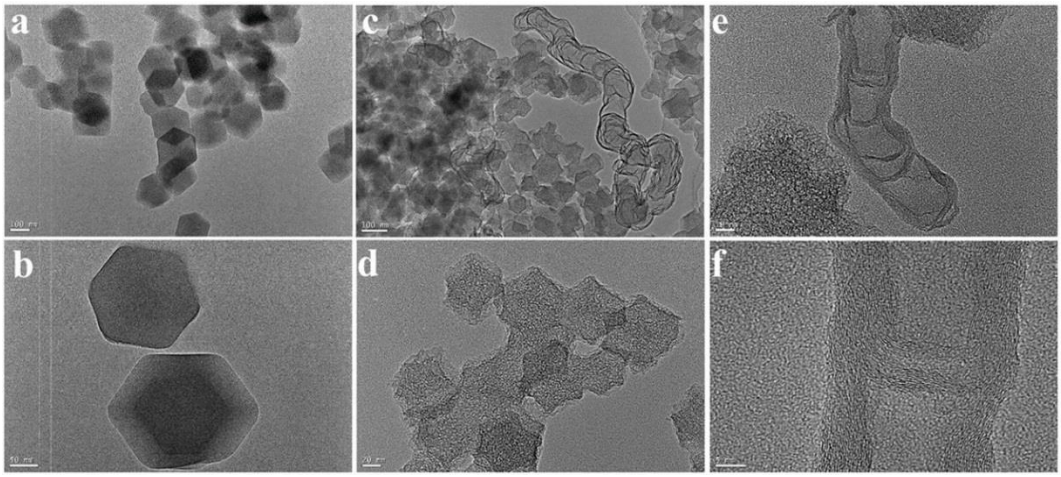

Figure S1. TEM images of (a)(b) ZIF-8@Fe-Co, (c)(d) APPC and (e)(f) generated carbon nanotubes during calcination. The scales are (a) 100 nm, (b) 10 nm, (c) 100 nm, (d) 20 nm, (e) 10 nm and (f) 5 nm, respectively.

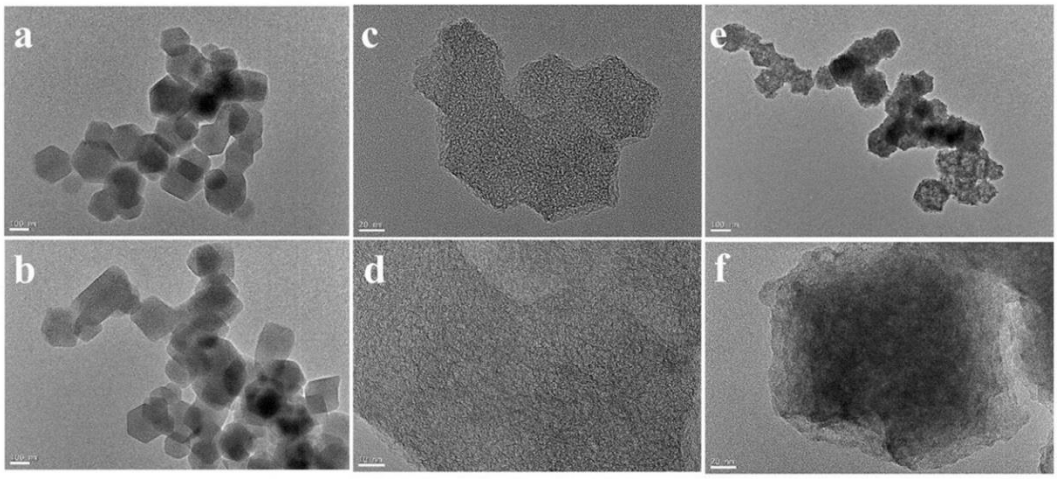

Figure S2. TEM images of (a)(b) ZIF-8, (c)(d) PC and (e)(f) PC/Se. The scales are: (a)(b)(e) 100 nm; (c)(f) 20 nm; (d) 10 nm.

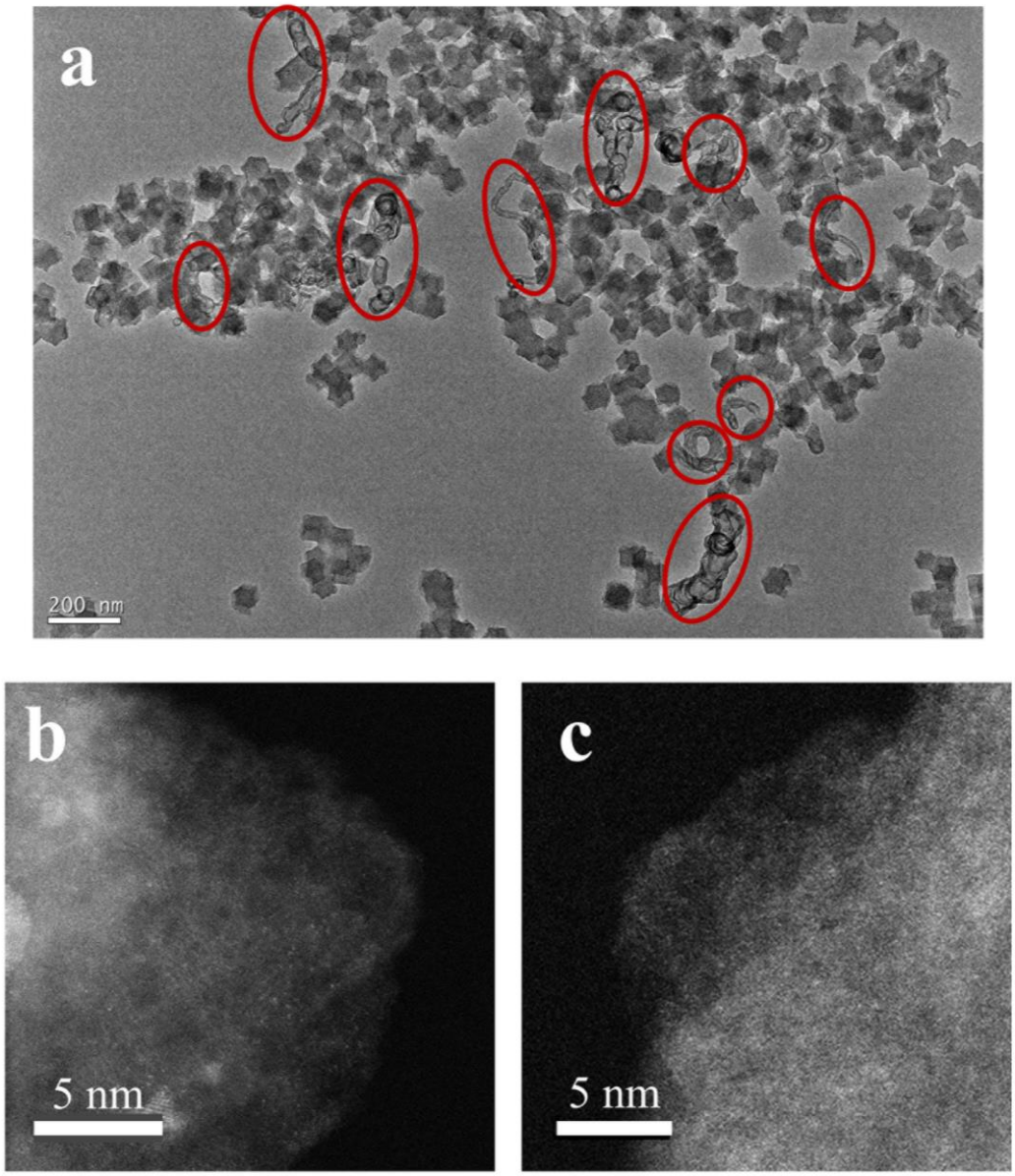

Figure S3. (a) TEM images of APPC and CNTs highlighted by red circles. (b) (c) Atomic-level HAADF-STEM images of APPC.

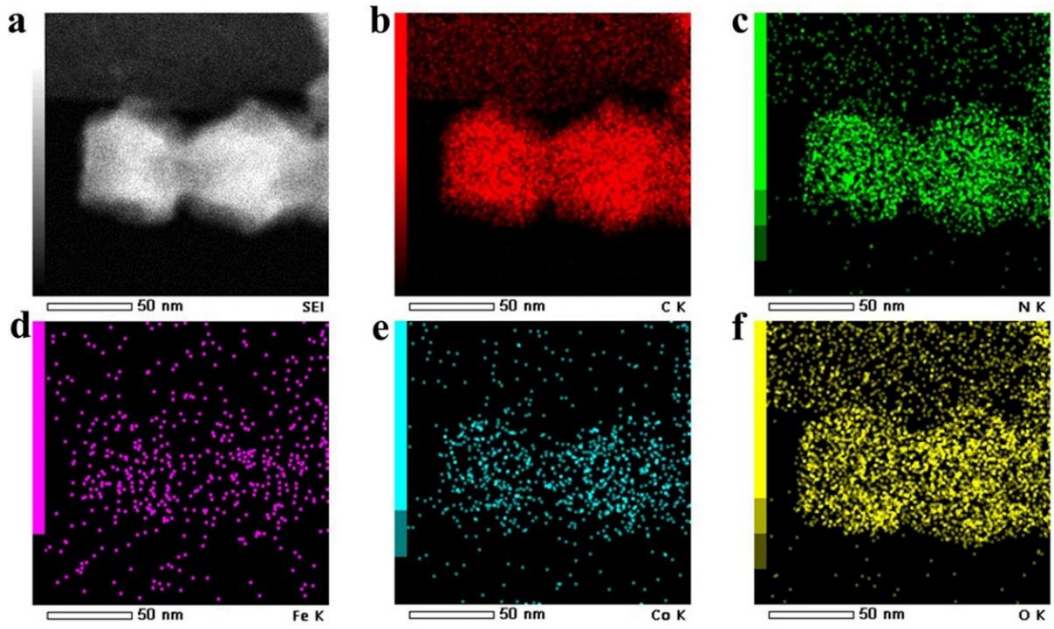

Figure S4. (a) STEM image of APPC and (b-f) EDS elemental maps of C, N, Fe, Co and O, respectively.

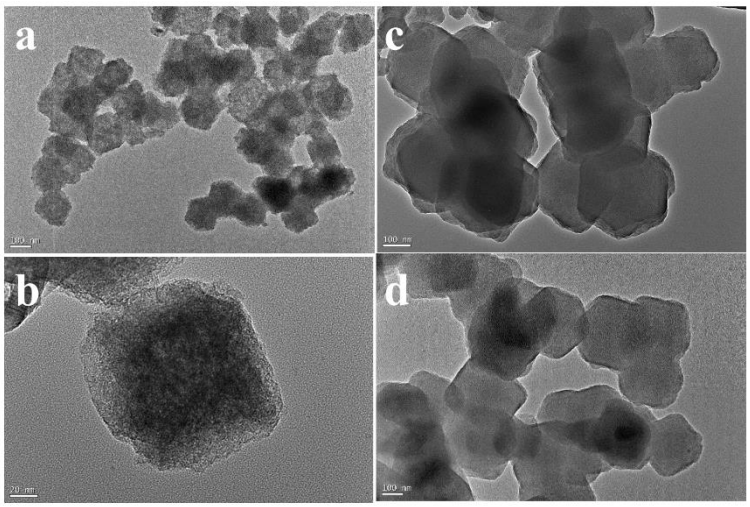

Figure S5. TEM images of (a)(b) APPC/Se, (c)(d) APPC/Se@PDA. The scales are 20 nm for (b), 100 nm for others, respectively.

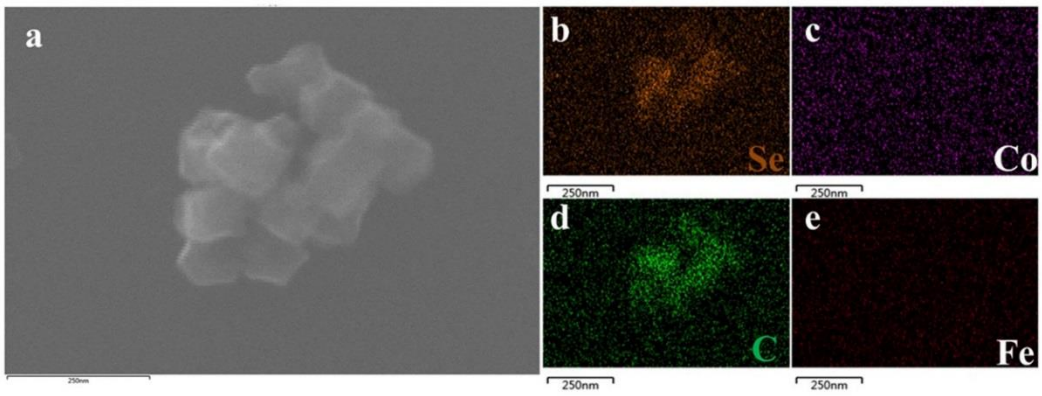

Figure S6. (a) SEM image of PC/Se and (b-e) EDS elemental maps of Se, Co, C and Fe, respectively. The scale of (a) is 250 nm.

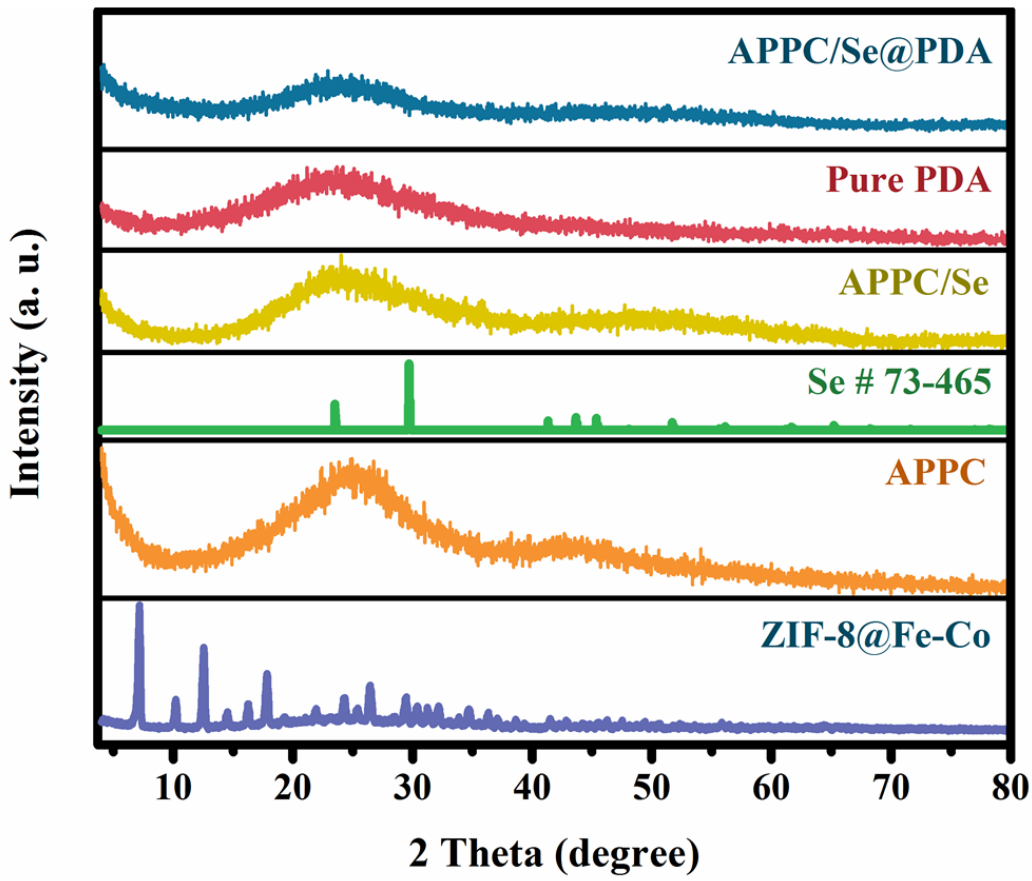

Figure S7. XRD patterns of APPC/Se@PDA, APPC/Se, APPC and pure PDA.

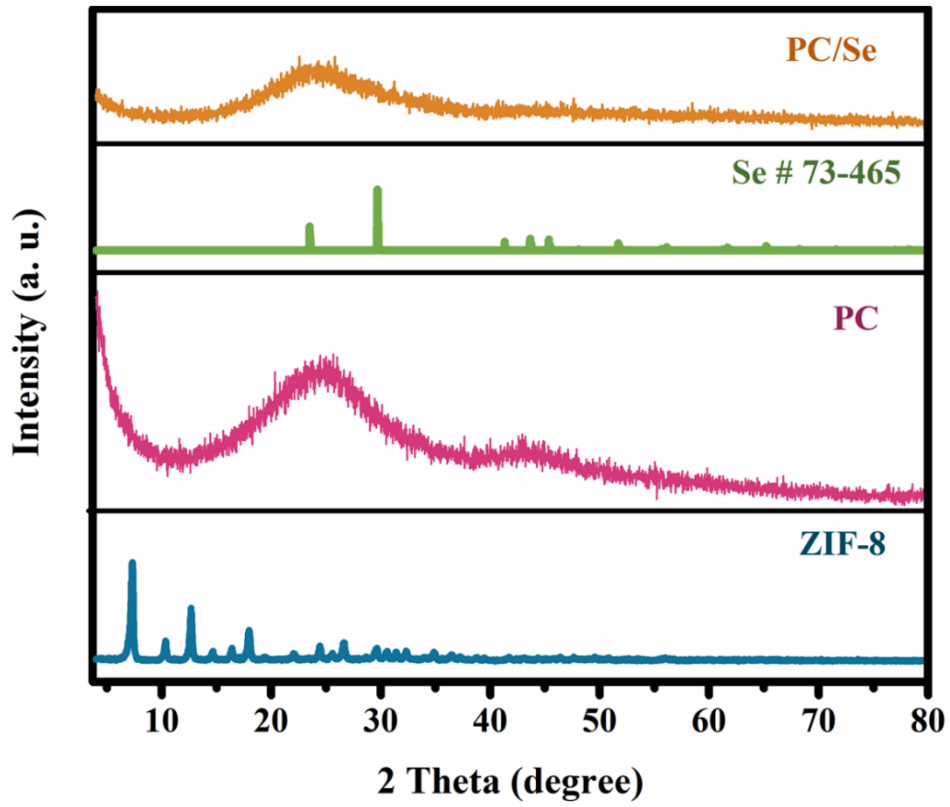

Figure S8. XRD paterns of ZIF-8, PC and PC/Se. pore size distributions using DFT analysis of PC and PC/Se, respectively.

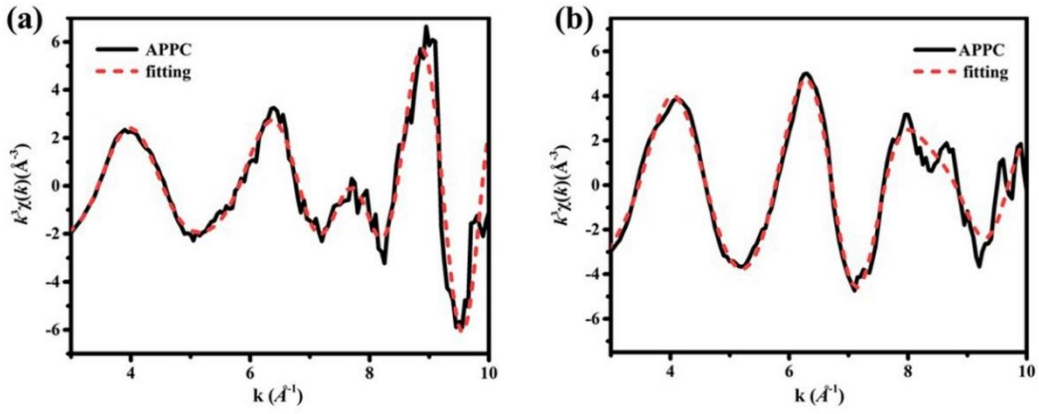

Figure S9. (a) Co K-edge EXAFS k-plot fitting curves and (b) Fe K-edge EXAFS k-plot fitting curves.

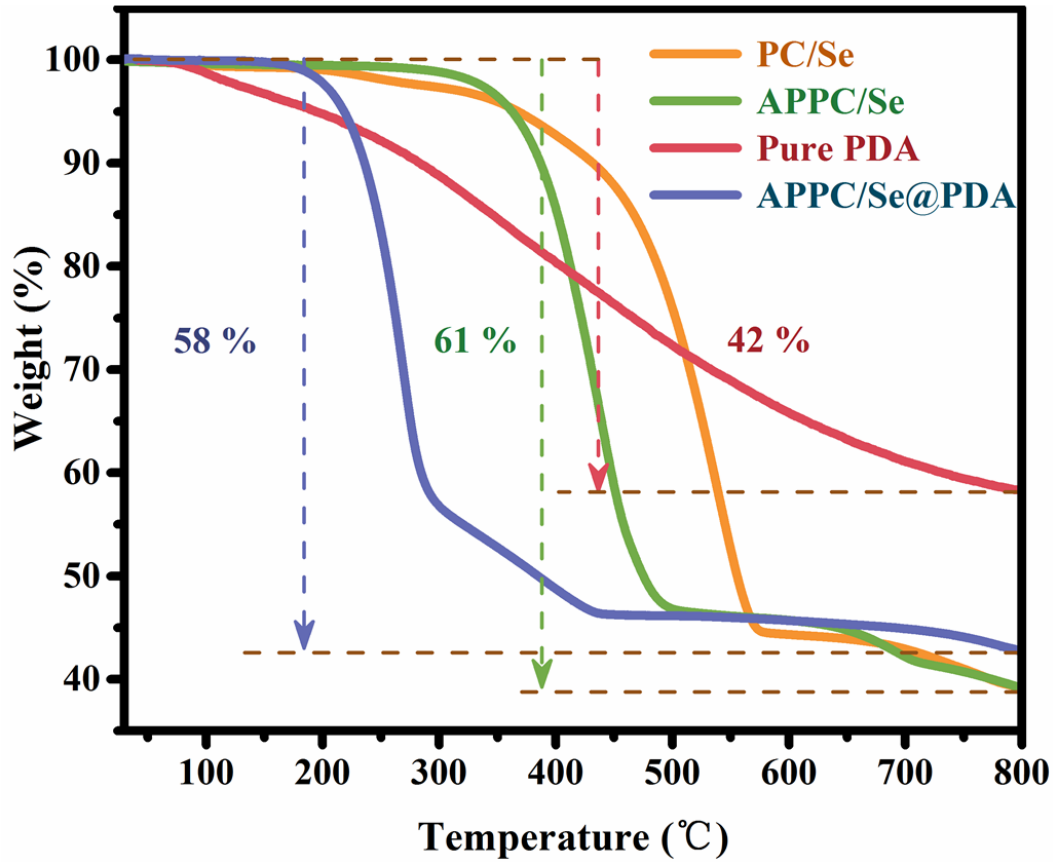

Figure S10. TG curves of APPC/Se@PDA, APPC/Se, PC/Se and pure PDA.

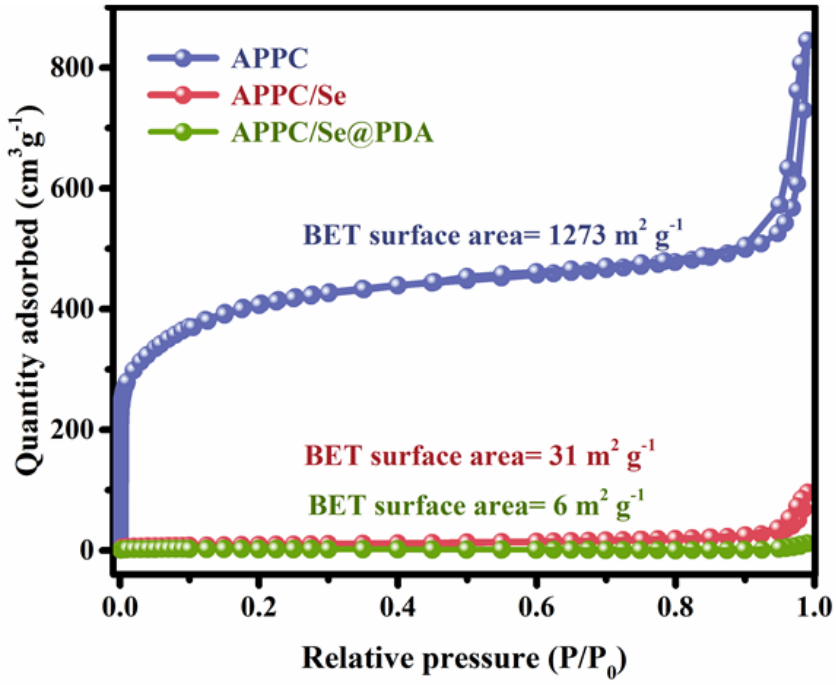

Figure S11. (a) N_2 adsorption-desorption isotherms of APPC, APPC/Se and APPC/Se@PDA.

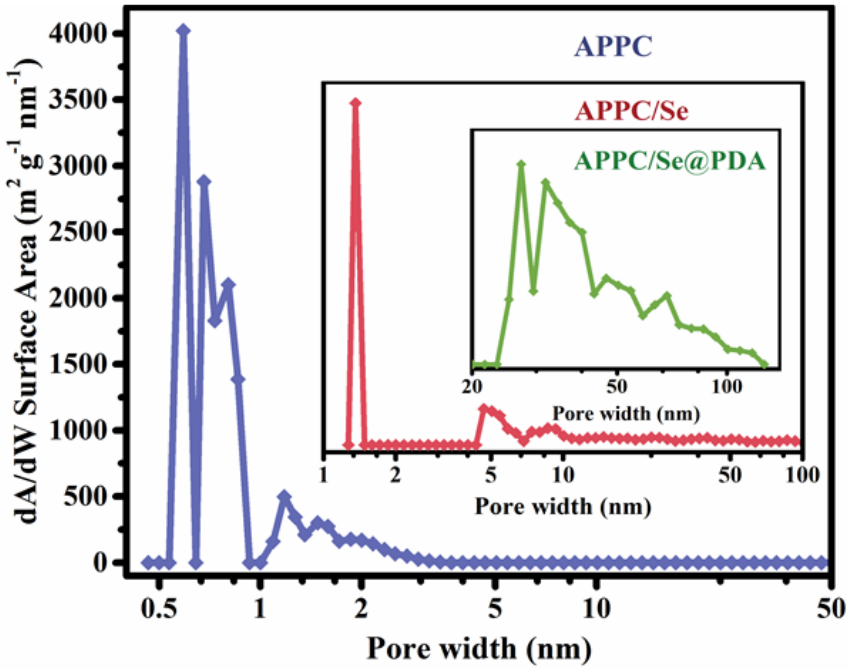

Figure S12. Pore size distributions using DFT analysis of APPC, APPC/Se and APPC/Se@PDA , respectively.

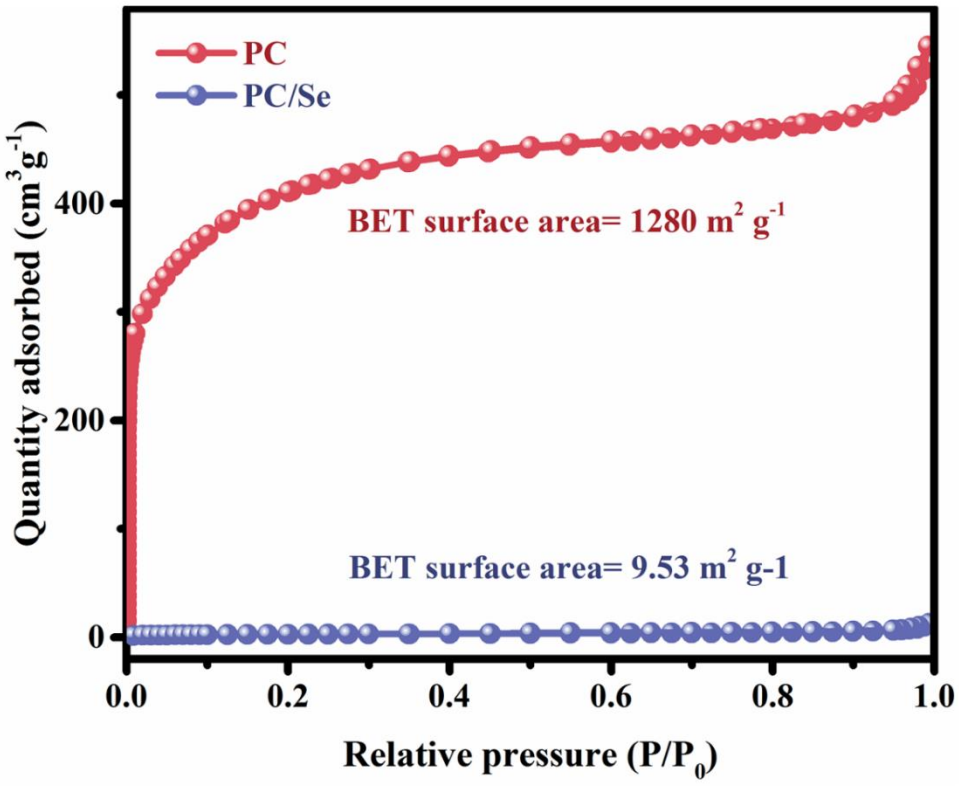

Figure S13. N_2 adsorption-desorption isotherms of PC and PC/Se.

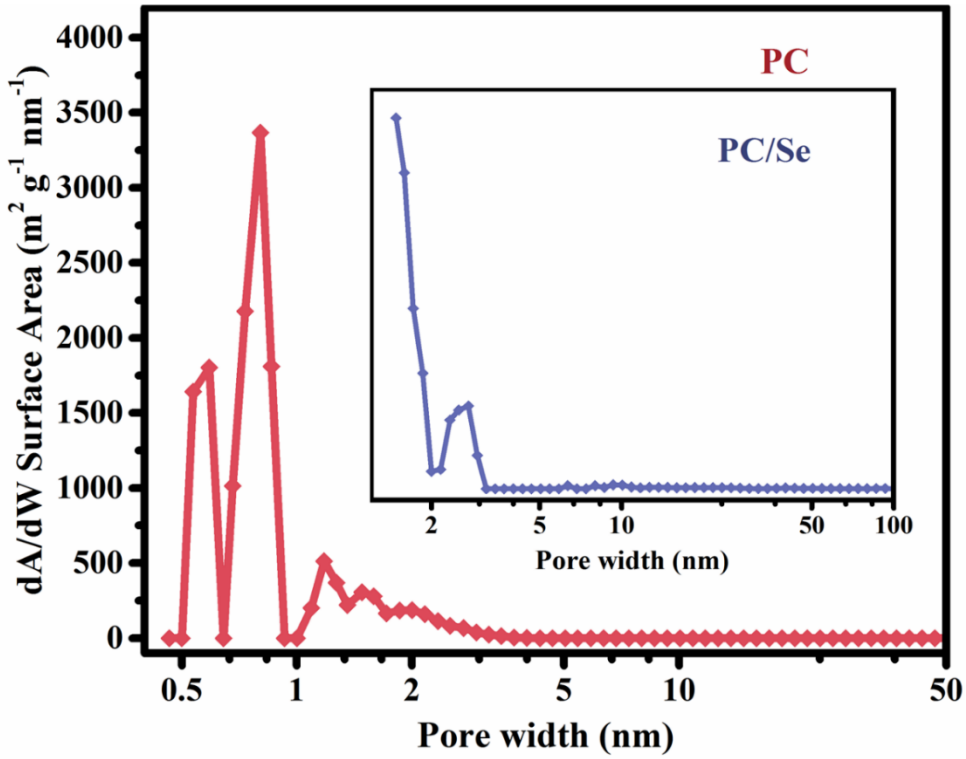

Figure S14. Pore size distributions using DFT analysis of PC and PC/Se.

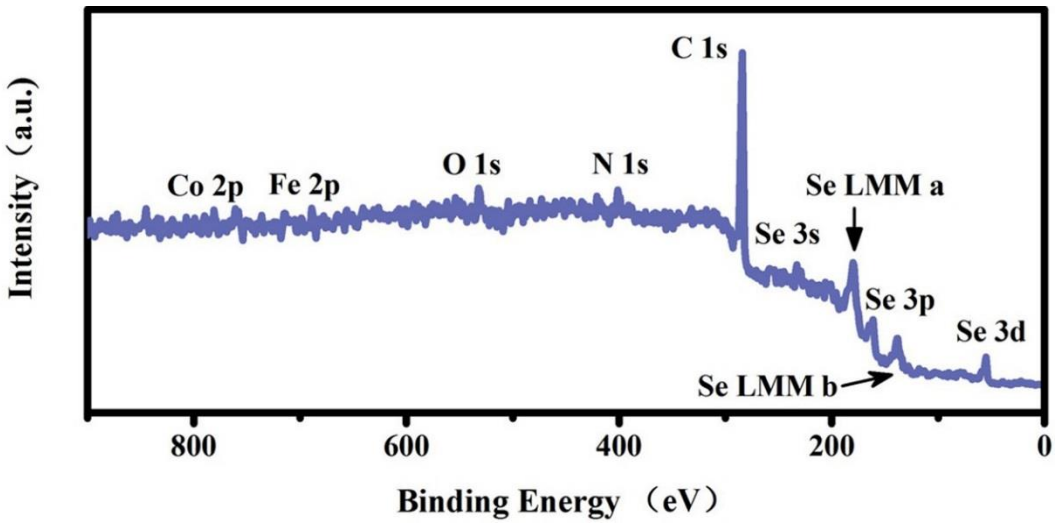

Figure S15. XPS survey spectra of APPC/Se.

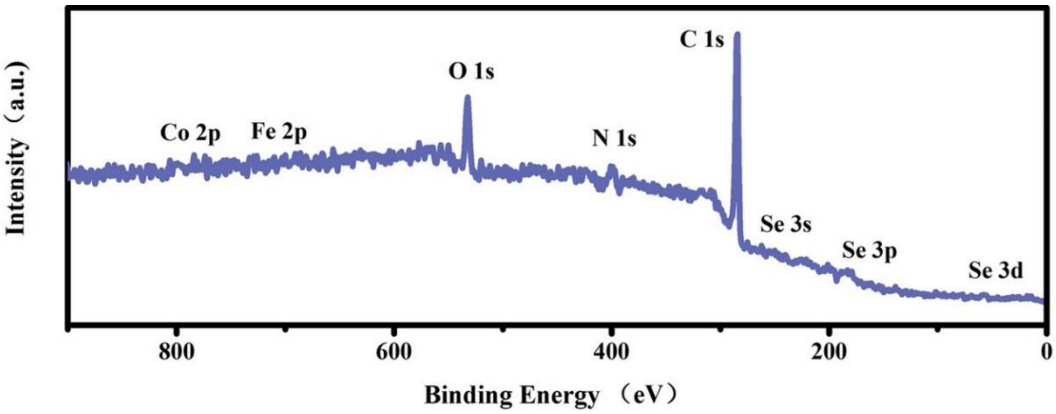

Figure S16. XPS survey spectra of APPC/Se@PDA.

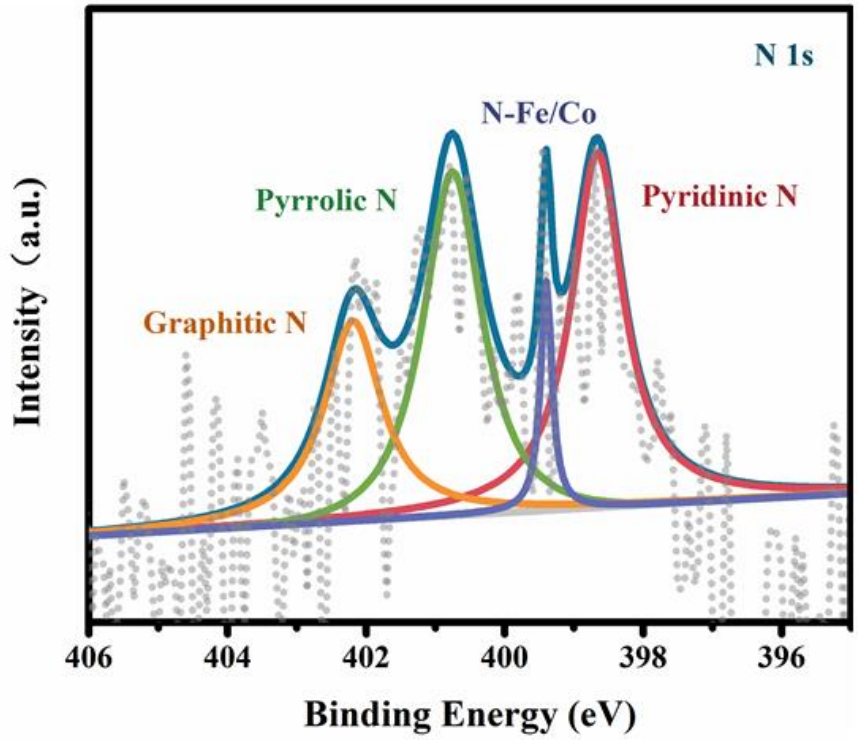

Figure S17. N 1s XPS survey spectra of APPC/Se.

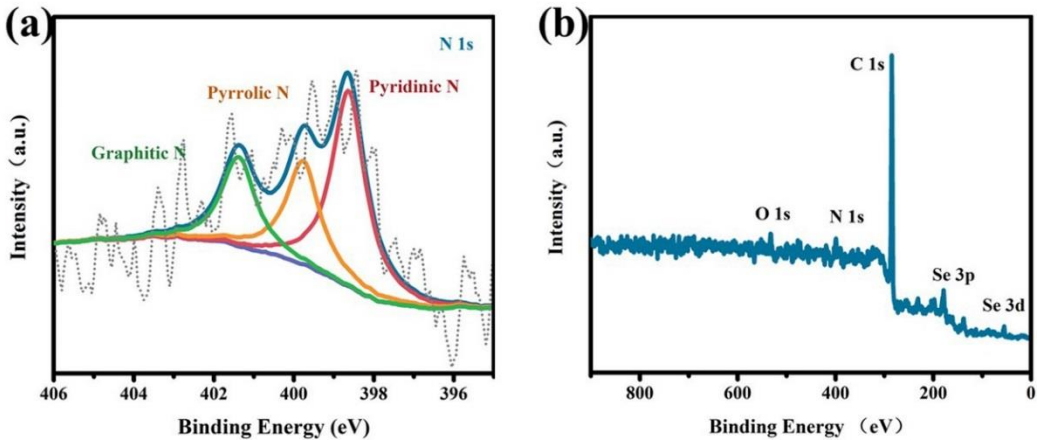

Figure S18. (a) N 1s and (b) XPS survey spectra of PC/Se.

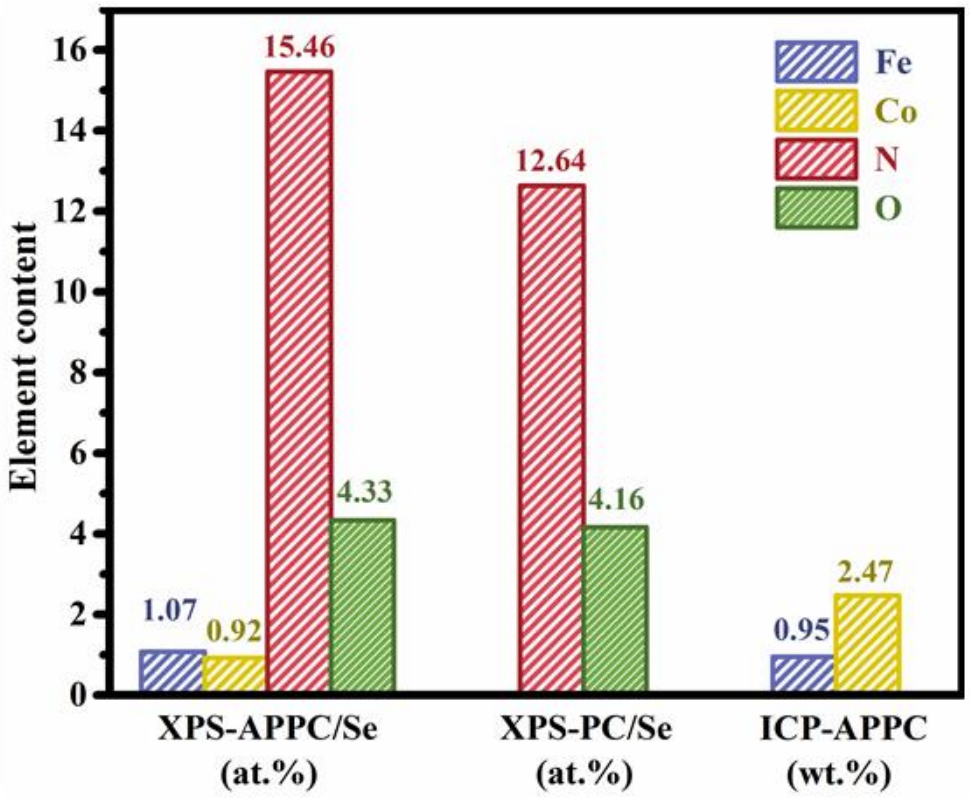

Figure S19. Element contents measured by XPS and Inductively Coupled Plasma Optical Emission Spectrometry (ICP-OES).

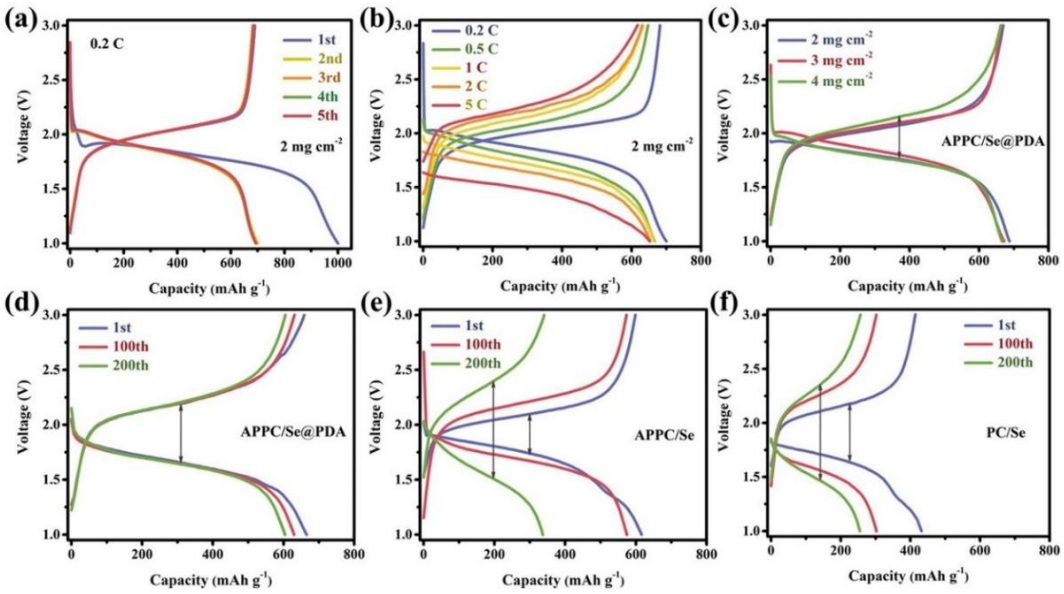

Figure S20. Typical voltage profiles of APPC/Se@PDA cathode (a) for 1-5 cycles at 0.2 C, (b) from 0.2 to 5 C at a selenium loading of 2 mg cm^{-2} and (c) at 0.5 C for three different Se loadings. Typical voltage profiles at 2 C for 1st cycle, 100th cycle and 200th cycle of (d) APPC/Se@PDA, (e) APPC/Se and (f) PC/Se cathodes at a Se loading of 2 mg cm^{-2}, respectively.

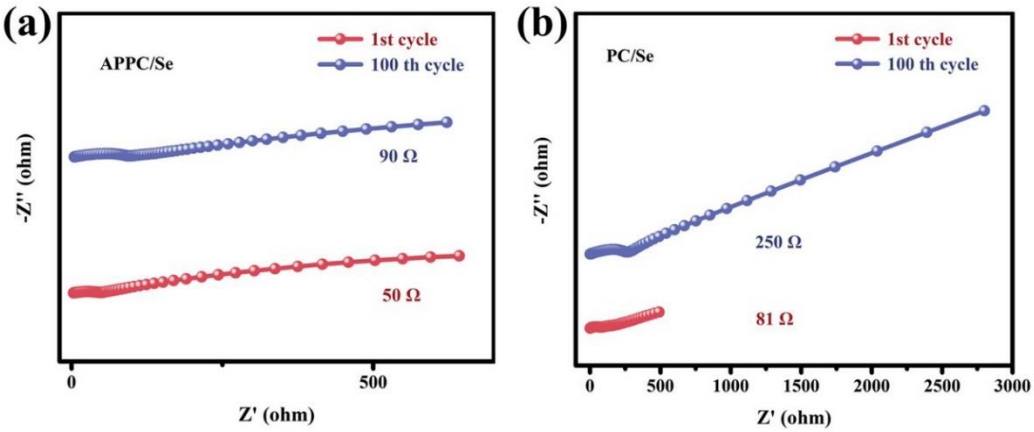

Figure S21. Nyquist plots of (a) APPC/Se and (b) PC/Se cathodes after 1 st cycle and 100th cycle, respectively.

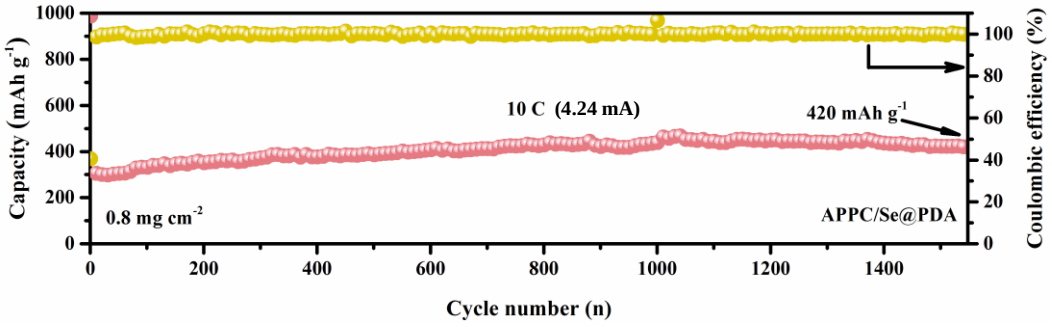

Figure S22. Cycling performance at 10 C of APPC/Se@PDA cathode.

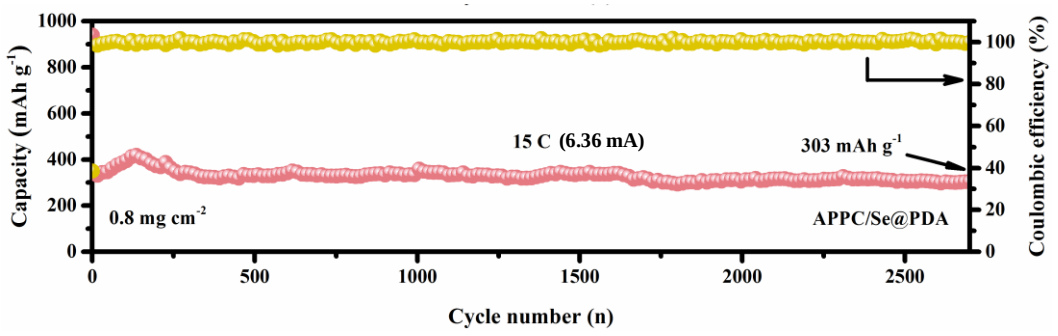

Figure S23. Cycling performance at 15 C of APPC/Se@PDA cathode.

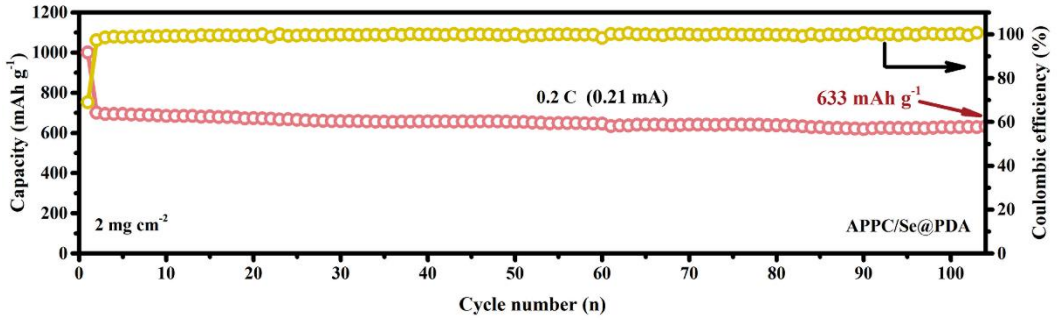

Figure S24. Cycling performance at 0.2 C of APPC/Se@PDA cathode at a Se loading of 2 mg cm^{-2}.

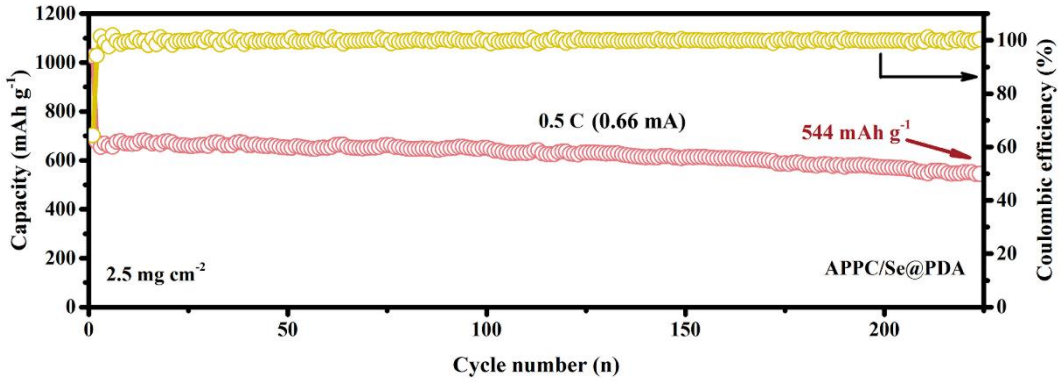

Figure S25. Cycling performance at 0.5 C of APPC/Se@PDA cathode at a Se loading of 2.5 mg cm^{-2}.

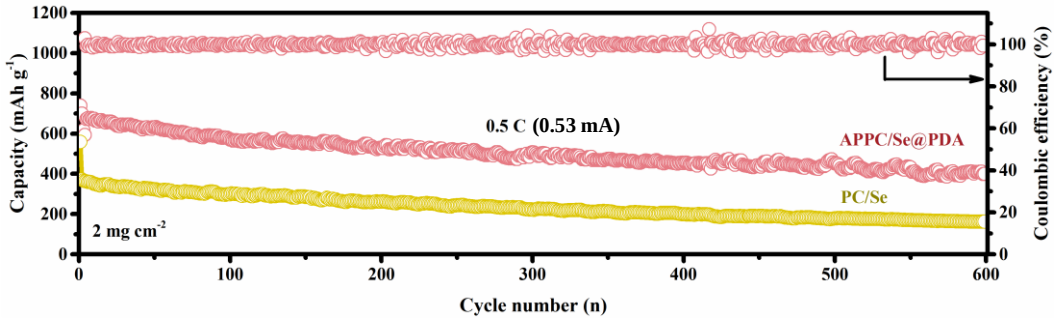

Figure S26. Cycling performance at 0.5 C of APPC/Se and APPC/Se@PDA cathodes.

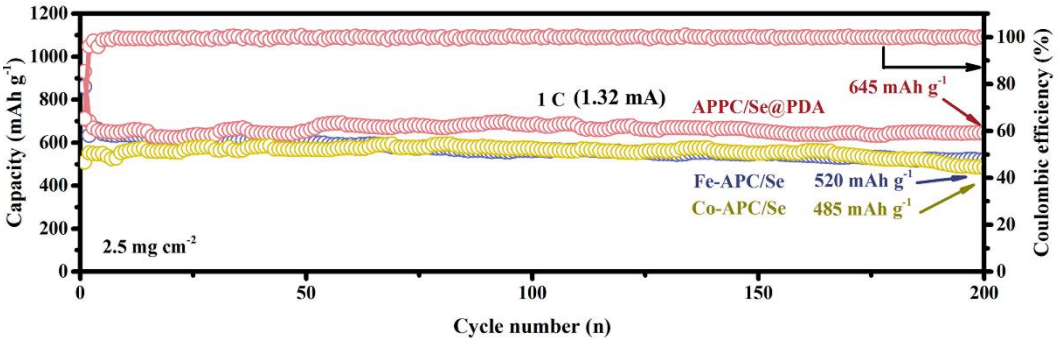

Figure S27. Cycling performance at 1 C of APPC/Se@PDA, Fe-APC/Se and Co-APC/Se cathodes at a Se loading of 2.5 mg cm^{-2}.

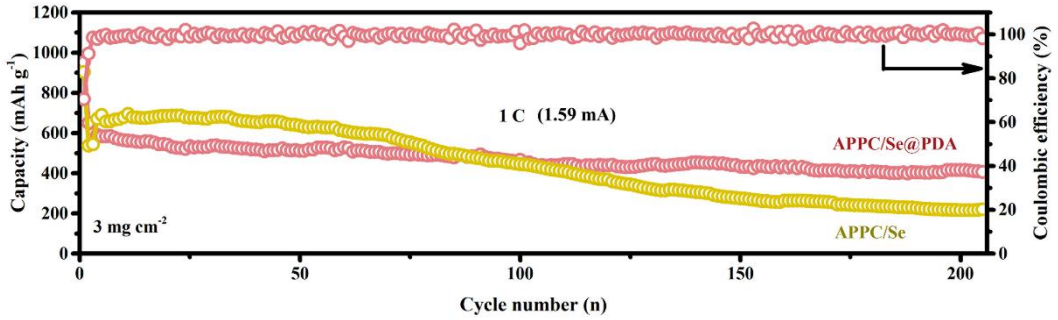

Figure S28. Cycling performance at 1 C of APPC/Se@PDA and APPC/Se cathodes at a Se loading of 3 mg cm^{-2}.

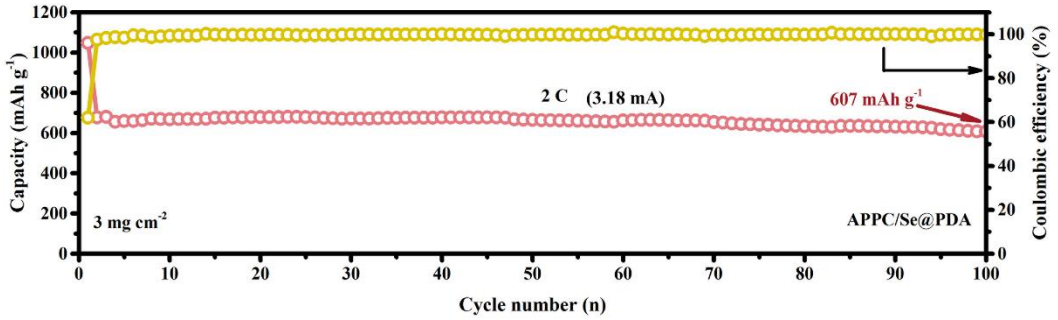

Figure S29. Cycling performance at 2 C of APPC/Se@PDA cathode at a Se loading of 3 mg cm^{-2}.

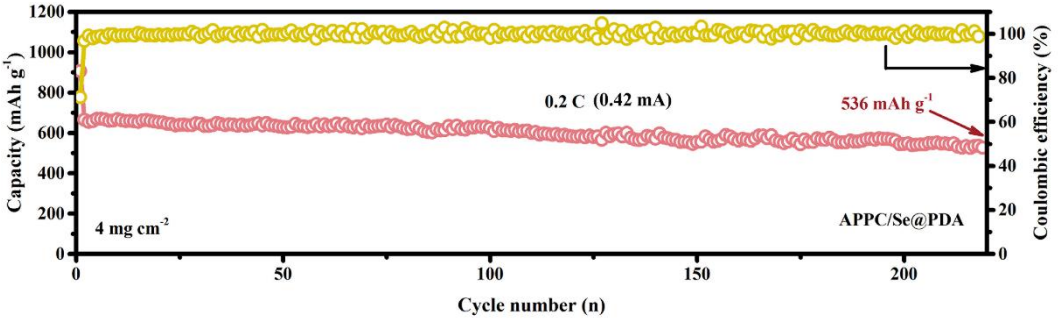

Figure S30. Cycling performance at 0.2 C of APPC/Se@PDA cathodes at a Se loading of 4 mg cm^{-2}.

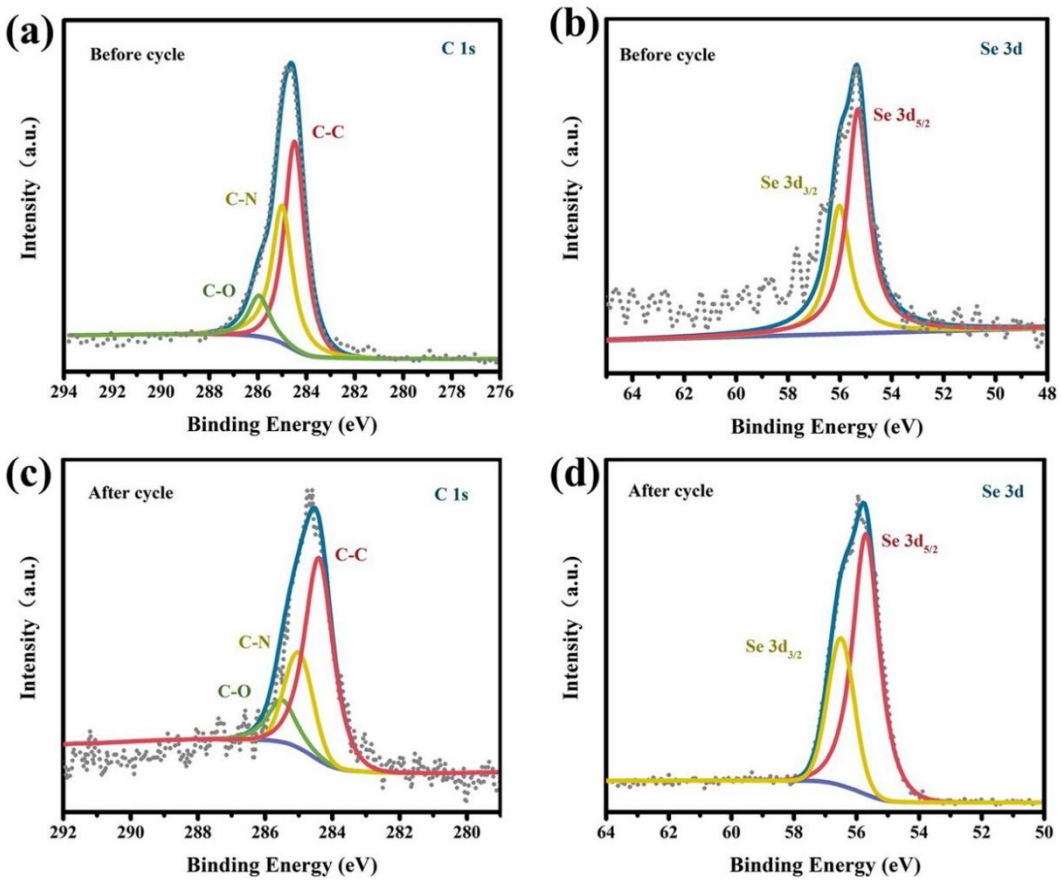

Figure S31. The ex-situ (a)(c) C 1s and (b)(d) Se 3d XPS spectra of PC/Se cathode.

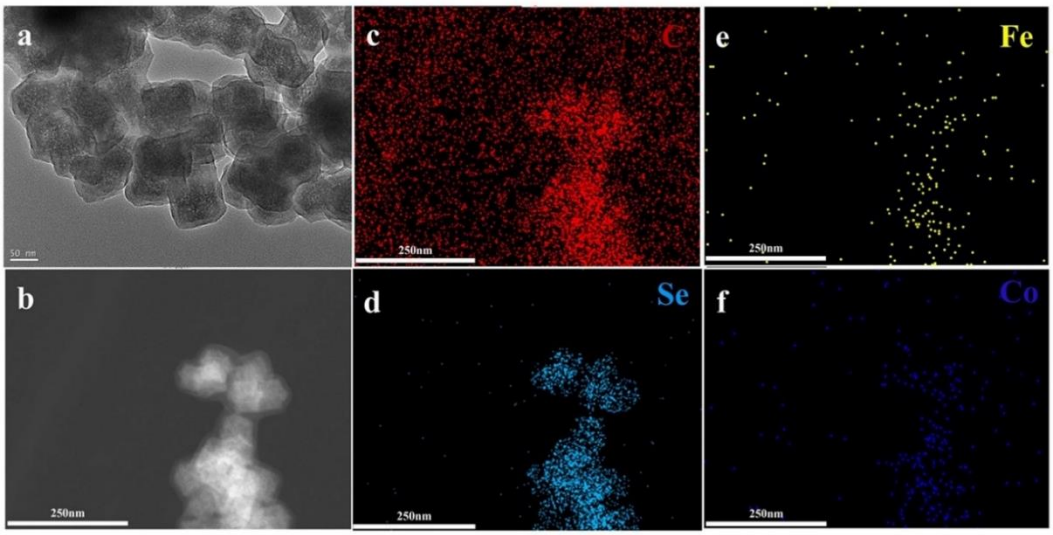

Figure S32. (a)(b)The TEM images of APPC/Se@PDA cathode after 600 cycles and (c) the EDS elemental mapping corresponding to (b).

Table S1. EXAFS data fitting results of APPC.

Edge	Path	N	R(Å)	σ^2(Å^2)
Fe	Fe-N_1	2	2.00	0.003
	Fe-N_2	2	2.09	0.004
Co	Co-N_1	2	1.94	0.003
	Co-N_2	1	2.00	0.003
	Co-Co	1	2.39	0.002

N: coordination number;

R: distance between absorber and backscatter atoms;

σ^2 : the Debye-Waller factor value.

Table S2. The calculation of selenium content in APPC/Se@PDA.

$W_{APPC/Se\ in\ APPC/Se@PDA}$	x
$W_{PDA\ in\ APPC/Se@PDA}$	y
$W_{Se\ in\ APPC/Se}$	61%
$W_{loss\ of\ pure\ PDA}$	42%
$W_{loss\ of\ APPC/Se@PDA}$	58%

From above we conclude that x+y=1 and 61%*x+42%*y=58%, so x=16% and y=84%.

As a result, the content of Se in APPC/Se@PDA is 84%*61%=51%.

Table S3. Comparison of electrochemical performance of various carbon hosts as Se cathodes reported for Li-Se batteries with the APPC/Se@PDA cathode in this work.

Samples	Se loading (mg cm^{-2})	Current density	Capacity (mAh g^{-1})	Cycle number	Ref.
APPC/Se@PDA	**0.8**	**2 C**	**645**	**700**	**This work**
		5 C	**500**	**1400**	
		10 C	**420**	**1500**	
		15 C	**303**	**2700**	
		23 C	**274**	**2500**	
	2	**0.5 C**	**400**	**600**	
	4	**0.2 C**	**536**	**220**	
Se@Co_{SA}-HC	0.8	5 C	340	1500	Ref.1
		20 C	237	2500	
A4-carbon/Se	0.4	3 C	343	2000	Ref.2
NPC/CGB-Se	0.4	15 C	409	10	Ref.3
	1.8	0.5 C	380	90	
MiC/Se	1.8	0.5 C	400	500	Ref.4
	2.2	0.5 C	348	500	
PANI@Se/C-G	2	0.2 C	588.7	200	Ref.5
		2 C	528.6	500	
		5 C	403	500	
BP-CNF/Se	0.4	0.5 C	588	300	Ref.6
Se–NCHPC	0.7	2 C	305	60	Ref.7
Se/MMPBc-3	1.3	0.2 C	467	300	Ref.8
Se–CP	-	1 C	506	150	Ref.9
Se/CMK-3	-	1 C	304	500	Ref.10
Se/MCN-RGO	1.2	1 C	385	1300	Ref.11
Se/CMCs	1	0.5 C	231	460	Ref.12
		2 C	166	460	

1. H. Tian, H. Tian, S. Wang, S. Chen, F. Zhang, L. Song, H. Liu, J. Liu and G. Wang, *Nat. Commun.*, 2020, **11**, 5025.
2. G. D. Park, J. H. Kim, J.-K. Lee and Y. Chan Kang, *J. Mater. Chem. A*, 2018, **6**, 21410-21418.
3. S. K. Park, J. S. Park and Y. C. Kang, *ACS Appl. Mater. Interfaces*, 2018, **10**, 16531-16540.
4. X. Wang, Y. Tan, Z. Liu, Y. Fan, M. Li, H. A. Younus, J. Duan, H. Deng and S. Zhang, *Small*, 2020, **16**, e2000266.
5. B. Wang, J. Zhang, Z. Xia, M. Fan, C. Lv, G. Tian and X. Li, *Nano Res.*, 2018, **11**, 2460-2469.
6. S.-K. Park, J.-S. Park and Y. C. Kang, *J. Mater. Chem. A*, 2018, **6**, 1028-1036.
7. Y. Qu, Z. Zhang, S. Jiang, X. Wang, Y. Lai, Y. Liu and J. Li, *J. Mater. Chem. A*, 2014, **2**, 12255-12261.
8. H. Zhang, F. Yu, W. Kang and Q. Shen, *Carbon*, 2015, **95**, 354-363.
9. Z. Yi, L. Yuan, D. Sun, Z. Li, C. Wu, W. Yang, Y. Wen, B. Shan and Y. Huang, *J. Mater. Chem. A*, 2015, **3**, 3059-3065.
10. C. P. Yang, S. Xin, Y. X. Yin, H. Ye, J. Zhang and Y. G. Guo, *Angew. Chem. Int. Ed.*, 2013, **52**, 8363-8367.
11. K. Han, Z. Liu, J. Shen, Y. Lin, F. Dai and H. Ye, *Adv. Funct. Mater.*, 2015, **25**, 455-463.
12. T. Liu, M. Jia, Y. Zhang, J. Han, Y. Li, S. Bao, D. Liu, J. Jiang and M. Xu, *J. Power Sources*, 2017, **341**, 53-59.